

Study of Third-Order Optical Nonlinearities of Substituted Hydrazones in PMMA

S. Vijayakumar,¹ Adithya Adhikari,² Balakrishna Kalluraya,² K. N. Sharafudeen,¹ K. Chandrasekharan¹

¹Laser and Nonlinear Optics Laboratory, Department of Physics, National Institute of Technology Calicut, Calicut-673601, India

²Department of Chemistry, Mangalore University, Mangalagangothri-574199, India

Received 17 April 2009; accepted 21 April 2010

DOI 10.1002/app.32691

Published online 27 July 2010 in Wiley Online Library (wileyonlinelibrary.com).

ABSTRACT: We investigated the third-order nonlinear optical properties of donor–acceptor substituted hydrazones doped into PMMA matrix using single beam Z-scan technique at 532 nm. The magnitude of third-order susceptibility, $\chi^{(3)}$ is of the order of 10^{-13} esu. The nonlinear refractive index, n_2 and the molecular second order hyperpolarisability, γ_h are of the order of 10^{-11} esu and 10^{-32} esu, respectively. The compounds exhibit larger

third-order NLO properties in PMMA host when compared to the pure compounds. The study reveals that these hydrazones are a good candidate of nonlinear optical materials for photonic applications. © 2010 Wiley Periodicals, Inc. *J Appl Polym Sci* 119: 595–601, 2011

Key words: nonlinear absorption; nonlinear refractive index; Z-scan; optical limiting

INTRODUCTION

Organic materials with large third-order nonlinear optical (NLO) properties will be the key elements for future photonic technologies because of their potential applications in all optical switching, data processing, and eye and sensor protection.^{1–3} The nonlinearity in organic materials originates from a strong delocalization of π electrons along the length of the molecules.^{4,5} With the aid of novel synthetic chemistry we are able to engineer the organic molecules by substituting them with strong electron donating and withdrawing entities and to enhance their optical nonlinearities.^{3,6}

Among the various organic compounds, hydrazones have revealed to be an important class of organic materials exhibiting the properties of various optics phenomena. Since the hydrazone backbone is an asymmetric transmitter, it strongly increases the molecular nonlinearity for the electron donating and withdrawing group substitutions.^{7–9} We selected a hydrazone derivative, ethyl 2-[(2E)-2-benzylidenehydrazino]-5-nitrobenzoate and substituted with it different electron donating groups. These compounds possess noticeable third-order nonlinearity. However, they cannot be used directly in practical applications because they are not flexible. Moreover they can get

degraded when exposed to intense laser light. To overcome these problems and make effective use of these materials in devices, they can be doped into a polymer matrix. This can enhance the opto-chemical and opto-physical stability, mechanical and thermal properties, and linear optical transparency.¹⁰

Here we report the results of our experiments using single beam Z-Scan technique to measure the third-order NLO properties of these hydrazones namely ethyl 2-[(2E)-2-benzylidenehydrazino]-5-nitrobenzoate (HZ-1), ethyl 2-[(2E)-2-(4-hydroxybenzylidene)hydrazino]-5-nitrobenzoate (HZ-2), ethyl 2-[(2E)-2-(4-methoxybenzylidene)hydrazino]-5-nitrobenzoate (HZ-3), and ethyl 2-[(2E)-2-(4-hydroxy-3-methoxybenzylidene)hydrazino]-5-nitrobenzoate (HZ-4) in Poly (methyl methacrylate) (PMMA) host. The optical limiting studies were also carried out.

PMMA has been selected as a matrix because it is hard, rigid but transparent polymer with glass transition temperature of 125°C. It is a polar material and has large dielectric constant. The physical durability of PMMA is far superior to that of other thermoplastic and is tougher than polystyrene.¹¹ Being an organic material it possess high optical and thermo mechanical damage resistant in the range needed for optical limiting applications.¹

Experiment

The compounds were synthesized by following the standard procedure.¹² The structures of the compounds are shown in Figure 1(a–d).

Correspondence to: K. Chandrasekharan (csk@nitc.ac.in).

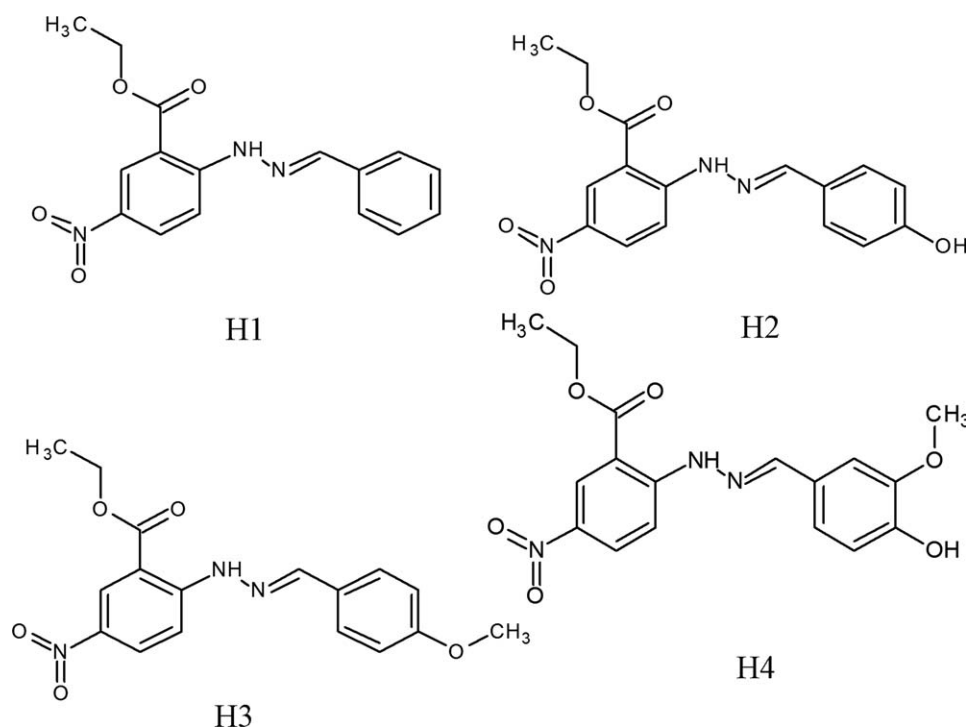


Figure 1 The chemical structures of the samples.

To prepare doped polymer samples, both the compounds and PMMA are dissolved separately at room temperature in dimethyl formamide (DMF). The solutions are then mixed and stirred slowly for an hour to get a uniform solution. The concentration of the dopant in PMMA matrix was varied from 5 to 25%. The linear absorption spectra of the samples recorded at room temperature in dilute DMF solution using a spectro photometer (UV-2500 PC Series) are shown in the Figure 2. The linear absorption spectrum of the PMMA doped solutions shows that all the compounds are transparent at 532 nm.

The linear refractive indices of the samples were measured using a Refracto 30GS digital refractometer. The measurements were performed on sample solutions of concentration 1×10^{-2} mol/L.

Z-scan measurements

The single beam Z-scan technique¹³ was used to study the nonlinear response of the samples. It is a simple but accurate method to determine both nonlinear refractive index (n_2) and nonlinear absorption coefficient (β_{eff}). By monitoring the transmittance through a small circular aperture placed at the far field position (closed aperture), one can determine the nonlinear refractive index. The nonlinear absorption coefficient of the sample can be determined using the open aperture (OA) Z-scan arrangement.^{13,14} A Q-switched Nd: YAG laser with a pulse width of 7 ns at 532 nm was used in the experiment.

A lens of focal length 30 cm was used to focus the laser pulses into a 1 mm-quartz cuvette containing sample solution. The closed aperture (CA) Z-scan was performed with 50% aperture. The input energy used was 50 μJ , which corresponds to a peak intensity of $1.13 \text{ GW}/\text{cm}^2$. The Z-scan measurements were performed on sample solutions of concentration 1×10^{-2} mol/L. In an attempt to suppress cumulative thermal effects, data were collected in single shot mode.¹⁵ Optical limiting studies were performed by keeping the sample at the focus by varying the input

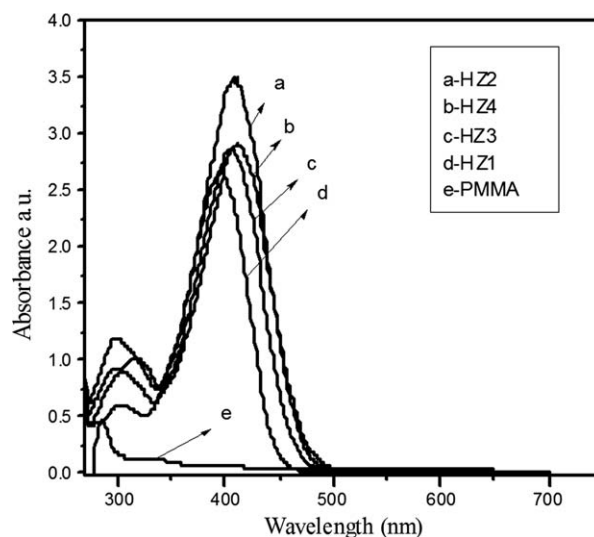


Figure 2 Linear absorption spectra of the samples in PMMA.

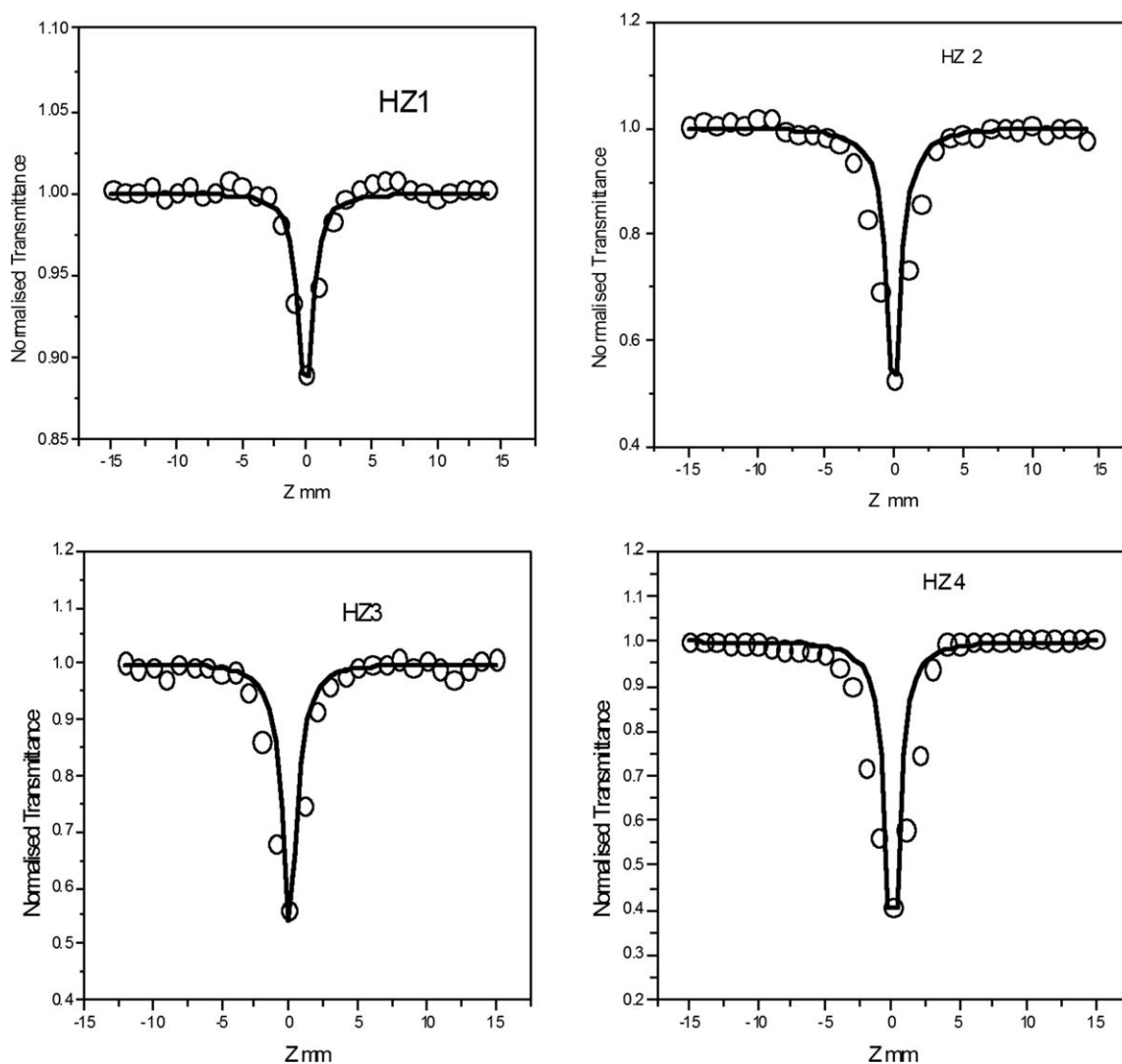


Figure 3 Open aperture Z-scan curves for the samples at $I_0 = 1.13 \text{ GW/cm}^2$. The solid line is fitted with (a) $\beta_{\text{eff}} = 1.55 \text{ cm/GW}$ for HZ-1, (b) $\beta_{\text{eff}} = 5.4 \text{ cm/GW}$ for HZ-2, (c) $\beta_{\text{eff}} = 4.2 \text{ cm/GW}$ for HZ-3 and (d) $\beta_{\text{eff}} = 6.8 \text{ cm/GW}$ for HZ-4.

energy and by monitoring the output energy. The incident and transmitted energies were measured simultaneously by two Rj-7620 energy ratio meters.

RESULTS AND DISCUSSION

The nonlinear transmission of the compounds with and without aperture was measured in the far field as the sample is moved through the focal point. Assuming a spatial and temporal Gaussian profile for laser pulses, the open aperture (OA) normalized energy transmittance is given by,^{13,16}

$$T_{\text{open}}(z) = \sum_{m=0}^{\infty} \frac{[-q_0(z,0)]^m}{(m+1)^{3/2}} \quad \text{with} \quad q_0(z,0) = \frac{\beta_{\text{eff}} I_0 L_{\text{eff}}}{1 + z^2/z_0^2}, \quad (1)$$

where β_{eff} is the effective two photon absorption coefficient, I_0 is the input irradiance, z is the sample

position, $z_0 = \pi\omega_0^2/\lambda$, is the Rayleigh range with ω_0 being the beam waist radius at the focal point ($z = 0$), L is the sample length, and λ is the laser wavelength. For fitting the data with eq. (1), we consider L_{eff} as the effective path lengths in the case of 2PA and is defined by $L_{\text{eff}} = 1 - e^{-\alpha_0 L}/\alpha_0$, where α_0 is the linear absorption coefficient.

Figure 3 shows the normalized transmission for OA Z-scan for the samples HZ-1, HZ-2, HZ-3, and HZ-4 in PMMA (concentration of 25% in matrix). Here the solid line is a theoretical fit of the experimental data to the eq. (1), which yields the value of effective two photon absorption (TPA) coefficient, β_{eff} .

To differentiate nonlinear refraction from nonlinear absorption, one can follow the division method.¹³ Figure 4 shows the pure nonlinear refraction curve obtained by dividing CA data by the corresponding OA data. The normalized transmittance for the pure nonlinear curves is shown to be

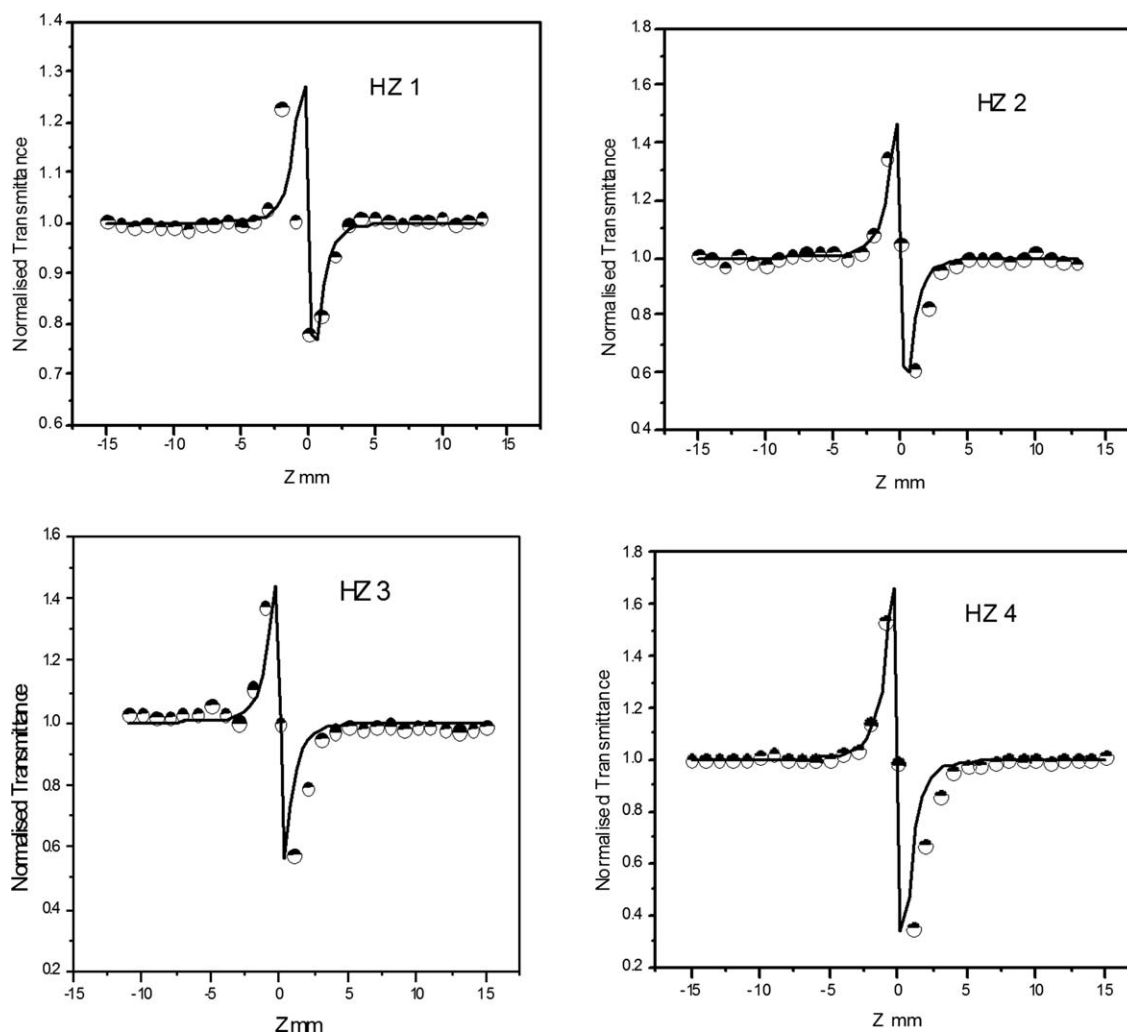


Figure 4 Pure nonlinear curves obtained by division method. Solid lines are theoretical fit of experimental data to eq. (2).

$$T = 1 - \frac{4\Delta\phi_0 x}{(x^2 + 1)(x^2 + 9)}, \quad (2)$$

where T is the normalized transmittance for the pure refractive nonlinearity, $\Delta\phi_0$ is the on-axis nonlinear phase shift at the focus and $x = z/z_0$.¹⁴

Now we can determine the real and imaginary part of the third-order nonlinear optical susceptibility $\chi^{(3)}$ according to the following relations;

$$\text{Re } \chi^{(3)} = 2n_0^2 \varepsilon_0 c \gamma, \quad (3)$$

$$\text{Im } \chi^{(3)} = n_0^2 \varepsilon_0 c \beta \lambda / 2\pi, \quad (4)$$

where n_0 is the linear refractive index, ε_0 is the vacuum permittivity, and c is the velocity of light in vacuum.¹³ γ is the nonlinear refractive index given by the formulae

$$\gamma = \frac{\Delta\phi_0 \lambda}{2\pi L_{\text{eff}} I_0}. \quad (5)$$

The nonlinear refractive index n_2 (esu) was calculated from the conversion formulae

$$n_2(\text{esu}) = \frac{cn_0\gamma}{40\pi}. \quad (6)$$

The calculated value of $\chi^{(3)} = \sqrt{(\text{Re}\chi^{(3)})^2 + (\text{Im}\chi^{(3)})^2}$ for the samples is of the order of 10^{-12} – 10^{-13} esu depending on different donor group substitutions. The value of n_2 is found to be of the order of 10^{-11} esu.

The coupling factor ρ , the ratio of imaginary part to real part of third-order nonlinear susceptibility can be measured as,

$$\rho = \text{Im } \chi^{(3)} / \text{Re } \chi^{(3)} = \beta / 2k\gamma. \quad (7)$$

The observed values of coupling factor for the samples HZ-1, HZ-2, HZ-3, and HZ-4 are -0.062 , -0.122 , -0.107 , and -0.106 , respectively.

The nonlinear induced polarization per molecule is described by the microscopic susceptibilities known

TABLE I
Linear and Nonlinear Optical Parameters of Hydrazone Derivatives in PMMA Host

	n_0	β_{eff} (cm/GW)	σ_2 (10^{-46}) ($\text{cm}^4\text{s}/\text{Photon}$)	n_2 (10^{-11} esu)	γ_h (10^{-32} esu)	$\text{Re } \chi^{(3)}$ (10^{-13} esu)	$\text{Im } \chi^{(3)}$ (10^{-13} esu)
HZ-1	1.425	1.55	0.960	-3.60	1.97	-3.88	0.241
HZ-2	1.458	5.40	3.346	-6.28	3.27	-7.01	0.884
HZ-3	1.426	4.20	2.603	-5.63	3.07	-6.03	0.646
HZ-4	1.426	6.80	4.210	-9.35	5.12	-10.02	1.070

as the hyperpolarizabilities.¹ For third-order effects the corresponding hyperpolarizability γ_h (second order hyperpolarizability) is related to the third-order susceptibility $\chi^{(3)}$ by the equation

$$\gamma_h = \frac{\chi^{(3)}}{\left[\frac{1}{3}(n_0^2 + 2)\right]^4 N}, \quad (8)$$

where N is the density of molecules in the unit of molecules per cm^3 and n_0 is the linear refractive index of the medium.^{17,18} The value of γ_h obtained is of the order of 10^{-32} esu, which is well comparable with the value reported for widely used thiophene oligomers by Hein et al. and chalcone derivatives investigated by John Kiran et al.^{17,19}

The two photon absorption cross section, σ_2 (in units of $\text{cm}^4\text{s}/\text{Photon}$), which defines the transition rate for TPA²⁰ was calculated for all the samples using the equation

$$\beta_{\text{eff}} = \sigma_2 N_A d \times 10^{-3}/h\nu, \quad (9)$$

where N_A is the Avogadro number, d is the concentration of the samples in mol/Liter and $h\nu$ is the energy of an incident photon (in Joules).^{21,22} It is observed that the TPA cross section increases with the electron donating ability of the substituents. The measured σ_2 values are in the order of $10^{-46}\text{cm}^4\text{s}/\text{photon}$. The calculated values of n_2 , β_{eff} , σ_2 , $\text{Re } \chi^{(3)}$, $\text{Im } \chi^{(3)}$, γ_h for the samples are shown in the Table I.

The $\text{Re } \chi^{(3)}$ values of the pure compounds HZ-1, HZ-2, HZ-3, and HZ-4 in the same experimental conditions are calculated to be -3.25×10^{-13} esu, -6.51×10^{-13} esu, -4.96×10^{-13} esu, and -9.5×10^{-13} esu, respectively. The nonlinear refractive index n_2 of the pure compounds HZ-1, HZ-2, HZ-3, and HZ-4 are -3.1×10^{-11} esu, -6.08×10^{-11} esu, -4.44×10^{-11} esu, and -8.83×10^{-11} esu, respectively. These results show that the compounds exhibit larger third-order NLO properties in PMMA host when compared to the pure compounds. The π electrons associated with the dopant molecules will form a cloud around the chain and can be distorted by applying an electric field, which results in to variation of nonlinear effects in the samples.

From the Table I it is clear that the nonlinear responses of the samples are influenced by the

strength of the electron donating substituents. The highest nonlinear response was observed with the sample HZ-4. In HZ-4, the hydroxy and methoxy group in the benzene ring (4-hydroxy and 3-methoxy group) are electron donating groups; whereas the nitro group (5-nitro group) and ester group are electron acceptors. Hence, there is a strong delocalization of electrons in the molecule that gives rises to the large nonlinear polarization. Consequently, the highest nonlinear response was observed with the sample HZ-4. In HZ-2, a hydroxy group (4-OH) is attached in the benzene ring while in HZ-3 a methoxy group (4-OCH₃) is attached. Since the hydroxy group is a stronger electron donor than methoxy group, we can expect an enhanced nonlinear response in HZ-2.

The excited state cross section σ_{ex} for all the samples can be determined from the procedure described in the literature.^{16,23} The σ_{ex} for the samples HZ-1, HZ-2, HZ-3, and HZ-4 are 0.445×10^{-18} cm^2 , 1.756×10^{-18} cm^2 , 1.59×10^{-18} cm^2 , and 1.9×10^{-18} cm^2 , respectively. The ground state absorption cross section σ_g can be calculated from the equation $\alpha = \sigma_g N_A C$ where N_A is the Avogadro number, C is the concentration in moles/ cm^3 and α is the linear absorption coefficient. The σ_g for the samples HZ-1, HZ-2, HZ-3, and HZ-4 are 6.64×10^{-21} cm^2 , 8.3×10^{-21} cm^2 , 3.32×10^{-21} cm^2 , and 31.37×10^{-21} cm^2 , respectively.

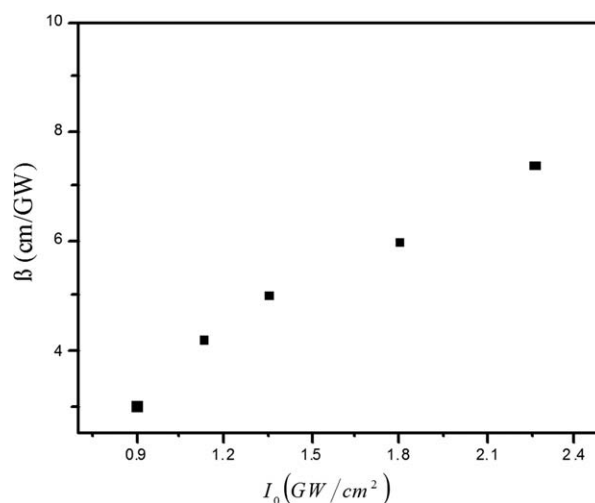


Figure 5 A plot of β_{eff} vs. I_0 for sample HZ-3.

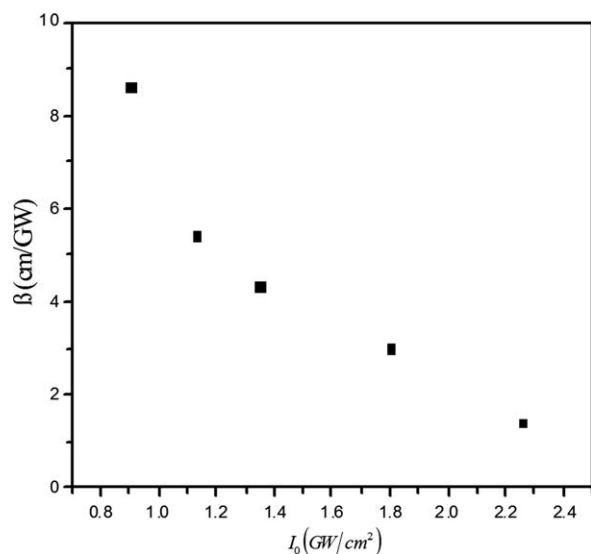


Figure 6 A fall of β_{eff} with increase in I_0 within the sample HZ-4.

The knowledge of the on-axis irradiance dependence of the nonlinear absorption (NLA) coefficient gives the information about the mechanism of the nonlinear absorption. Generally nonlinear absorption can be caused by free carrier absorption, saturable absorption, and direct multiphoton absorption or excited state absorption. If the mechanism belongs to the simple two photon absorption (TPA), β_{eff} should be a constant that is independent of the on-axis irradiance I_0 .²⁴ However, in compounds HZ-1 and HZ-3 (substituted with methoxy group) we find that β_{eff} increases with increase in I_0 and the intercept on the vertical axis is non-zero and the excited state absorption cross section is greater than the ground state absorption cross section. This suggests that a higher-

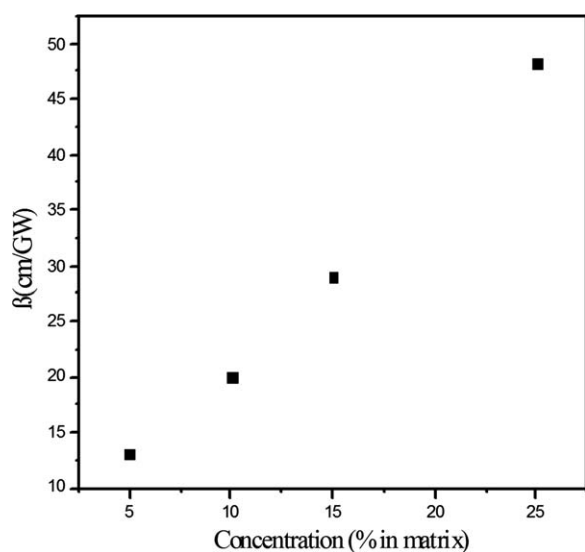


Figure 7 The dependence of β_{eff} on the concentration of the sample HZ-4 in the PMMA.

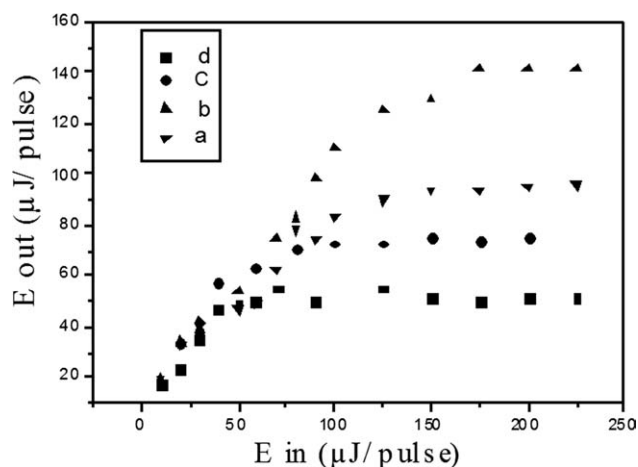


Figure 8 Optical limiting behavior in samples (a) HZ-3, (b) HZ-1, (c) HZ-2, and (d) HZ-4.

order effect, such as excited state absorption (ESA) accessed via two photon absorption, is contributing to the NLA.²⁵ However, a decrease of β_{eff} with I_0 was observed for the compounds HZ-2 and HZ-4. The fall of β_{eff} with increasing I_0 and the large value of σ_{ex} compared to σ_{g} are a consequence of reverse saturation absorption (RSA).²⁶ The responses of β_{eff} with I_0 for the samples HZ-3 and HZ-4 are as shown in the Figures 5 and 6, respectively. The dependence of β_{eff} on the concentration of the sample HZ-4 in the polymer matrix is shown in the Figure 7.

The optical limiting experiment was performed by keeping the sample at the focus. The input pulse energy steadily increased and output energy was recorded. Figure 8 shows the optical limiting behavior of the samples at 532 nm. It can be seen that the best limiting behavior is observed with HZ-4, which exhibits strongest nonlinear absorption among the samples. For input energies well below 250 μJ , there is no damage observed in the samples. However, beyond 300 μJ there is a deviation from the optical limiting behavior. It could be due to damage of sample with laser pulses.

CONCLUSIONS

The third-order nonlinear properties of donor-acceptor substituted hydrazone derivatives in PMMA matrix have been investigated by single beam Z-scan technique at 532 nm. The results show that these hydrazones exhibit larger third-order NLO properties in PMMA host when compared to the pure compounds. Good optical limiting behavior was observed in all the samples at 532 nm. The calculated values of nonlinear refractive index (n_2) and second order hyperpolarisability (γ_n) are of the order of 10^{-11} esu and 10^{-32} esu, respectively. Hence these hydrazones can be considered as a good class

of nonlinear optical dopant materials for optical device applications.

Authors wish to thank Dr. Reji Philip, Raman Research Institute, Bangalore, India and Dr. John Kiran, Ajou University, Suwon, South Korea, for their valuable suggestions to finalize this article.

References

1. Hari Singh Nalwa; Siezo Miyata. *Nonlinear Optics of Organic Molecules and Polymers*; CRC Press, Inc: USA, 1997.
2. Li, C.; Zhang, L.; Yang, M.; Wang, H.; Wang, Y. *Phys Rev A* 1994, 49, 1149.
3. Kiran, A. J.; Chandrasekharan, K.; Rai Nooji, S.; Sasikala, H. D.; Umesh, G.; Kalluraya, B. *Chem Phys* 2006, 324, 699.
4. Marder, S. R.; Torruellas, W. E.; Blanchard-Desce, M.; Ricci, V.; Stegeman, G. I.; Gilmour, S.; Bredas, J.-L.; Li, J.; Bublitz, G. U.; Boxer, S. G. *Science* 1977, 276, 1233.
5. Munn, R. W.; Ironside, C. N., Eds. *Principles and Applications of Nonlinear Optical Materials*; Chapman and Hall, CRC Press, London, 1993.
6. Zhan, X.; Liu, Y.; Zhu, D.; Huang, W.; Gong, Q. *J Phys Chem B* 2002, 106, 1884.
7. Serbutoviez, C.; Bosshard, C.; Knopfle, G.; Wyss, P.; Pretre, P.; Gunter, P.; Schenk, K.; Solari, E.; Chapuis, G. *Chem Mater* 1995, 7, 1198.
8. Wong, M. S.; Meier, U.; Pan, F.; Gramlich, V.; Bosshard, C.; Gunter, P. *Adv Mater* 1996, 8, 416.
9. Pan, F.; Wong, M. S.; Bosch, M.; Bosshard, C.; Meier, U. *Appl Phys Lett* 1997, 71, 2064.
10. Samoc, M.; Samoc, A.; Luther-Davis, B. J. *Opt Soc Am B* 1998, 15, 817.
11. Billmeyer, F. W. *Text Book of Polymer Science*, 3rd ed.; John Wiley and Sons: Singapore, 1994.
12. Furniss, B. S.; Hannaford, A. J.; Smith, P. W. G.; Tatchell, A. R. *Vogel's Textbook of Practical Organic Chemistry*, 5th ed.; Pearson Education: Singapore, 2005.
13. Sheik-Bahae, M.; Said, A. A.; Wei, T. H.; Hagan, D. J.; Van Stryland, E. W. *IEEE J Quant Electron* 1990, 26, 760.
14. Sheik-Bahae, M.; Said, A. A.; Van Stryland, E. W. *Opt Lett* 1989, 14, 955.
15. Yang, P.; Xu, J.; Ballato, J.; Schwartz, R. W.; Carroll, D. L. *Appl Phys Lett* 2002, 80, 3394.
16. Sutherland, R. L. *Handbook of Nonlinear Optics*; Dekker: New York, 1996.
17. Hein, J.; Bergner, H.; Lenzner, M.; Rentsch, S. *J Chem Phys* 1994, 179, 543.
18. Zhao, M. T.; Singh, B. P.; Prasad, P. N. *J Chem Phys* 1988, 89, 5535.
19. John Kiran, A.; Satheesh Rai, N.; Chandrasekharan, K.; Kalluraya, B.; Rotermund, F. *Jpn J Appl Phys* 2008, 47, 6312.
20. Robert W. Boyd. *Nonlinear Optics*, 2nd ed; Academic Press: USA, 2003.
21. He, G. S.; Weder, C.; Smith, P.; Prasad, P. N. *IEEE J Quantum Electron* 1998, 34, 2279.
22. Sutherland, R. L.; Brant, M. C.; Heinrichs, J.; Rogers, J. E.; Slagle, J. E.; Mclean, D. G.; Fleitz, P. A. *J Opt Soc Am B* 2005, 22, 1939.
23. Henari, F. Z.; Blau, W. J.; Milgrom, L. R.; Yahioglu, G.; Philips, D.; Lacey, J. A. *Chem Phys Lett* 1997, 267, 229.
24. Guo, S.-L.; Xu, L.; Wang, H. T.; You, X. Z.; Ming, N. B. *Optik* 2003, 114, 58.
25. Said, A. A.; Wamsley, C.; Hagan, D. J.; Van Stryland, E. W.; Reinhardt, B. A.; Roderer, P.; Dillard, A. G. *Chem Phys Lett* 1994, 228, 646.
26. Couris, S.; Koudoumas, E.; Ruth, A. A.; Leach, S. *J Phys B: At Mol Opt Phys* 1995, 28, 4537.